Tail length estimation from sacro-caudal skeletal morphology in catarrhines

AUTHOR(S):

TOJIMA, SAYAKA

CITATION:

TOJIMA, SAYAKA. Tail length estimation from sacro-caudal skeletal morphology in catarrhines. Anthropological Science 2013, 121(1): 13-24

ISSUE DATE:

2013-04

URL:

http://hdl.handle.net/2433/174129

Title: Tail length estimation from sacro-caudal skeletal morphology in catarrhines.

Author's name: Sayaka Tojima

Institution: Laboratory of Physical Anthropology, Graduate School of Science, Kyoto University, Kyoto 606-8502, Japan

Number of text pages: 28; Number of figures: 2; Number of tables: 5.

Keywords: last sacral vertebra; evolution of catarrhines; tail reduction

Corresponding author: Sayaka Tojima

Address: Kitashirakawa-Oiwake-cho, Sakyo, Kyoto 606-8502, Japan.

Phone: +81-75-753-4094

Fax: +81-75-753-4083

E-mail: tojima@anthro.zool.kyoto-u.ac.jp

Grant sponsorships: Supported by the Cooperation Research Program of the Primate Research Institute, Kyoto University, Inuyama, and by the Global COE Program A06 of Kyoto University, Japan.

ABSTRACT

Tail morphology in primates is important for interpreting functional adaptation and phylogeny. Tail length is probably the most remarkable trait. Establishing usable methods to predict the tail length of extinct primates is a part of the basis to reconstruct primate evolution, particularly of hominoids. Previous studies revealed that sacral morphology often predicts tail length. However, most of the previous studies have only attempted this by using categories (e.g., short, long, etc.). A problem in those studies is that the range of intermediate tail length is wide (whose tail length is 15.0 through100 percent of head to body length (15.0 < RTL < 100.0 %)). Accordingly, this study aimed to quantitatively estimate tail length in catarrhines with intermediate tail lengths. Sacral and proximal caudal vertebral (first to third) of 89 hybrid individuals between Japanese macaque (*Macaca fuscata*) and Formosan rock macaque (*Macaca cyclopis*) were measured. Fifteen regression formulae were produced to estimate tail length in these species. These hybrid macaques were phylogenetically controlled but varied greatly in their relative tail length (tail length / head and body length = 18.8 - 88.8%), and thus were an excellent sample to obtain general regression formulae to estimate catarrhine tail length. A total of 15 predicting models were devised and five formulae performed well. The utility of these formulae were confirmed by an application to 15 species/subspecies of catarrhine taxa.

INTRODUCTION

Tail length in primates varies greatly between species or even among local conspecific populations (Fooden, 1975, 1988, 2006; Napier and Napier, 1967; Napier, 1981; Hamada *et al.*, 2005, 2008a; also see Table 1). Thus, tail length is an important trait for understanding primate adaptation and phylogeny, for example thermoregulation (Wilson, 1972; Fooden and Albrecht, 1999), balance in arboreal activity (Wilson, 1972; Larson and Stern, 2006) in old world monkeys, and tail suspension or prehensility in new world monkeys (Cant *et al.*, 2001, 2003; German, 1982; Lemelin, 1995; Organ, 2007, 2010; Rosenberger, 1983; Schmitt *et al.*, 2005; Youlatos, 1998, 2002). In primates, the tail is markedly reduced in several lineages (e.g., apes, some macaques, lorises, some subfossil lemurs), but the evolutionary process and adaptive significance of tail reduction has not been thoroughly established. It is, therefore, important to obtain a reliable estimate of tail length from partial skeletal elements for the fossils of extinct primates.

Previous attempts addressed this issue using categorical methods. Ankel (1965, 1972) estimated tail length from the sacrum. She calculated the sacral index and explored the relationship between this index and tail length variation based on different numbers of caudal vertebrae. The sacral index devised in her study evaluated the relative development of neural tissue at the caudal sacral canal opening compare to the cranial canal opening. Twenty-one primate species (three species of prosimians, five species of platyrrhines, and 13 species of catarrhines including hominoids) were classified into several groups (e.g., “totally reduced tail,” “reduced tail” and “prehensiled tail” (in her 1972’s study, “tailless forms”, “long-tailed primates”, and “prehensile-tailed forms”

were used)). The sacral index successfully distinguished these groups, which had different tail lengths and different numbers of caudal vertebrae. The index value in "reduced tail" became smaller than longer tailed species, because reducing tail requires minimal innervations. Using this index, she also suggested that *Pliopithecus* (*Epipliopithecus*), a middle Miocene catarrhine from Europe, had a pendant "long-tail" (the index values were above those for "reduced tail" and below those for "prehensiled tail") that consisted of 10 to 15 caudal vertebrae (Ankel, 1965, 1972) though the interpretation that *Pliopithecus* was tailless was dominant (Zapfe, 1958). Ward *et al.* (1991) devised a tapering index of the sacrum and applied it to the sacrum of *Proconsul heseloni*, an early Miocene hominoid from western Kenya, and concluded that it had lost their tail. Their tapering index was calculated from the cranial, caudal width and the vertebral body length of the last sacral vertebra, and tailess primate had a larger tapering index because the caudal end articulated with vestigial coccygeal vertebra rather than a robust Ca1. Nakatsukasa *et al.* (2003, 2004) also investigated taillessness in Miocene hominoids by using different criteria, like the shape of transverse process or trabecular mesh, and concluded that *Nacholapithecus kerioi* (Nakatsukasa *et al.*, 2003) and *Proconsul heseloni* (Nakatsukasa *et al.*, 2004) also lacked tails.

Recently, Russo and Shapiro (2011) clarified the relationships between sacral morphology and relative tail length (RTL = tail length/head and body length *100 %) in catarrhines. They classified 22 catarrhine taxa into four groups: "long" (100.0 % ≤ RTL), "short" (37.0 ≤ RTL < 100.0 %), "very short" (0.0 < RTL < 15.0 %), and "absent" (RTL = 0 %; hominoids). The study tested a utility of sacral measurements to distinguish these four groups. Three parameters concerning the shape of the sacral caudal articular surface, the sacro-caudal articulation angle (Schmitt *et al*, 2005) and the lateral

expansion of the transverse processes varied between these categories. Among these features, the sacro-caudal articulation angle (Schmitt *et al*, 2005) distinguished three groups, "long", "short" and "very short" groups, separately. The other features were useful to separate "long" and "tailless" groups from the "short"/"very short" groups although the study did not distinguish "short" and "very short" groups. Russo and Shapiro (2011) provided useful results for interpreting primate tail length. However, "short"-tailed group in their study still covers a broad range of tail length (37.0% ≤ RTL < 100.0%) and correlations between these parameters and RTL are low within each group. This study built on these previous results with the intention of estimating primate tail length with greater precision.

Specifically, this study aimed to devise reliable formulae for predicting the RTL quantitatively from the sacrum and proximal caudal vertebrae by using a phylogenetically narrow catarrhine sample (hybrid individuals of Japanese macaque and Formosan rock macaque). The study then tested the broader utility of the predictive formulae by applying the functions to 15 catarrhine species/subspecies other than Japanese and Formosan rock macaques (Table 1).

MATERIALS AND METHODS

Devising prediction models of relative tail length

This study collected predictive measurements from the skeletal specimens of hybrid Japanese macaques (*Macaca fuscata*) and Formosan rock macaques (*Macaca cyclopis*). The skeletal specimens are housed at the Primate Research Institute of Kyoto University. The two species express close phylogenetic relatedness but have significantly different

tail lengths (Fooden, 2006). Tail lengths and numbers of caudal vertebrae in these hybrids vary greatly depending on the degree of hybridization (Hamada *et al.*, 2008b). Additional components of morphological variability such as inter-temporal distance (Mouri *et al.*, 2008) and the size of incisors and molars (Kunimatsu and Yamamoto, 2008) also vary between these two species. Although *M. fuscata* and *M. cyclopis* are allopatrically distributed, the artificial introduction of *M. cyclopis* into Japan has caused sporadic hybridization in a certain region. About 50 years ago, a troop of *M. cyclopis* escaped from an abandoned private zoo park in Wakayama prefecture. The domesticated macaques then merged with wild local troops of *M. fuscata* and began to produce fertile offspring (Kawamoto *et al*, 1999, 2001; Ohsawa *et al*, 2005). As the population of hybrid macaques increased, the local government eradicated the groups to prevent further anthropogenic genetic disturbance in the wild *M. fuscata* populations following the Guidelines of Wild Life Management set by the Ministry of Environment. The captured macaques were euthanized.

Eighty-nine of these adult specimens were selected. The term adult references full emergence of the third molar. Their RTLs (tail length/head and body length (sitting height) x 100) were calculated using somatometrical tail length and sitting height from the cadavers (Hamada *et al*, 2008b). Generally, RTL is calculated from tail length and head and body length, however, head and body length were not measured in the hybrid samples. About this matter, Dr. Hamada said that the difference between head and body length and sitting height is lesser than 5% in the hybrids and the intraspecies RTL difference was much bigger (personal communication in 2011). Therefore in this study, the author decided to use sitting height instead of head and body length. RTLs of the adult hybrids varied from 18.3 % to 88.8 % (from 101 to 470 mm in tail length).

Table 1 around here

Twenty linear measurements were collected from the sacrum and the first to third caudal vertebrae (Ca1-Ca3) using digital sliding calipers with an accuracy of 0.1 mm (Mitsutoyo Co., Ltd.) (Figure 1). Previous studies have revealed that the caudal end of the sacrum which was measured relative to the cranial end tends to reflect tail length strongly (Ankel, 1965, 1972; Ward *et al*., 1991; Russo and Shapiro, 2011). Six measurements from the caudal side of the sacrum including the measurements used in the previous studies (measurements No.5 and 6 from Ankel (1965, 1972); measurements No. 7, 8, and 11 from Russo and Shapiro (2011); measurements No.12 is original in this study, see Figure 1) were, therefore collected. In addition, 14 measurements on the cranial and caudal sides of the sacrum were also collected. For example, measurements No.1, 2, 5, 6 are used to calculate Ankel's sacral index (Ankel, 1965, 1972). Sacral breadth was measured at three different levels and the total sacral length was measured. Generally, the measurements taken from the caudal side of the sacrum decreased when tail length became shorter. The Ca1-Ca3 are readily identified morphologically even from isolated fossilized materials and were used in this study. More distal caudal vertebrae are identifiable only in cases where a substantial number of caudal vertebrae are associated.

In order to devise a set of RTL prediction formulae, these measurements were standardized in two different ways and selected for performance of the multiple regression analyses. The following rule was used for the strength of correlations in this study: $0.5 \leq r < 0.7$ was defined as a moderate positive correlation and $r \geq 0.7$ was

defined as a strong correlation (Sokal and Rohlf, 1995).

1. Standardization of measurements

To predict RTL, body size effects must be removed from the measurements. I standardized the measurements by the geometric mean of the cranial articular surface of the sacrum, which was calculated as (GMscra = (measurements No. 3 x No. 4)$^{0.5}$) (Figure 1). GMscra was correlated strongly with the head and body length (r = 0.74), but poorly with tail length (r = -0.43). Measurements were divided by GMscra.

2. Selection of variables from the standardized measurements

The correlation matrix of the standardized measurements (except measurements No. 3 and 4, which were used for size standardization) and RTL was calculated (Table 2). Measurements that show a low correlation (r < 0.5) with RTL were eliminated from further steps of the analyses. Then, in order to avoid multicolinearity in the multiple regression analysis, pairs of measurements that show a high correlation with each other (r>0.7) (Table 2) were selected and the term that expressed the weaker correlation with RTL was dropped. The remaining standard measurements were used for multiple regression analysis.

3. Multiple regression analyses

Using all remaining variables, multiple regression analysis was calculated. Akaike's information criterion (Akaike, 1973) was used to select the best multiple regression model by a step-wise method (backward/forward). A step-wise method does backward/forward steps (increasing/decreasing variables) from a full model (the model using all variables the performer chooses) and chooses the variables that make the F-value or p-value the largest.

4. Reducing variables from the devised regression formulae and obtaining new models

Other models were calculated by eliminating some measurements of some bony elements or bony parts from the regression formulae devised by the step-wise method. This operation was conducted under the assumption that various different elements or parts were preserved in fossil specimens. For example, no fossil specimens contain intact sacra and proximal caudal vertebrae, and even though sacra or caudal vertebrae are preserved, the neural arch and transverse processes are often broken.

Figure 1 around here

In the second analysis, indices that are empirically expected to reflect tail development were calculated. Several indices or angles were calculated from sacral measurements that were previously used to evaluate tail length (Ankel, 1965, 1972; Ward *et al*., 1991, Russo and Shapiro, 2011). Ankel (1965, 1972) demonstrated that the size of the caudal opening of the sacral canal is larger relative to the cranial opening in long-tailed primates. The sacral index she used was defined as: (No. 5 x No. 6)/ (No. 1 x No. 2) (Figure 1). Ward *et al*. (1991) also reached a similar conclusion based on the analysis of the sacral tapering angle to show that *Proconsul* did not have a tail. In other words, Ankel (1965, 1972) and Ward et al (1991) showed that the development of the morphology of sacral caudal end compare to the cranial end reflects tail length well. Russo and Shapiro (2011) calculated ML/DV ratios (mediolateral breadth of the last sacral vertebra's articular surface divided by its dorsoventral breadth (measurements No.7/No.8 in Figure 1)). Likewise, this study calculated 18 indices from paired measurements of the corresponding cranial and caudal elements (Table 2). The study focused on six measurements on the caudal side of the sacrum (measurements No. 5, 6,

7, 8, 11, and 12), which likely reflect tail development and divided them by their corresponding cranial measurements. These indices included ones suggested in the previous studies (TDSC (transverse diameter of the sacral canal), SDSC (sagittal diameter of the sacral canal) were from Ankel (1965, 1972); MLDV (mediolateral and dorsoventral breadth of the articular surface of the last sacral vertebra) was from Russo and Shapiro (2011)). The indices were used for multiple regression analyses following the same procedures as noted above (Table 4).

Table 2 around here

Determination of the relative contribution of each variable

In order to determine the relative contribution of each variable to the prediction models, standard partial regression coefficients (SPRCs) were calculated. SPRCs were calculated by multiplying unstandardized coefficients by the ratio between the standard deviation of each independent variable and the standard deviation of the dependent variable.

Examination of the applicability of models

The utility of the predicting formulae was tested by applying the results to 15 catarrhine species/subspecies other than Japanese and Formosan rock macaques (Table 1). Apes were not included in the samples because the number of sacral vertebrae and caudal vertebrae are greatly different between extant apes and the monkeys. The prediction formulae were calculated from the hybrid macaques possessing three sacral vertebrae. Therefore, these formulae are designed for “monkey-like” specimens with

three or four sacral vertebrae (as per: Zapfe 1958). This purported shortcoming does not limit the utility of this study in reconstructing tail reduction process in hominoid evolution. In fact, Rose et al. (1996) inferred that the tailless *Nacholapithecus kerioi* had a fewer number of sacral vertebra like monkeys from the sacral morphology. This is also supported by a greater number of lumbar vertebrae. Among the comparative cercopithecid samples, skeletons associated with individual RTL records were limited to six species/subspecies: *Cercopithecus mitis kolbi*, *C. mitis stuhlmanni*, *C. neglectus*, *C. aethiops*, *Papio anubis*, *Colobus guereza* were associated with the field record; RTLs of *M. arctoides* and *Cercocebus torquatus* were directly measured from the associated skin. For seven other species, the RTL was obtained from the literature: *Erythrocebus patas*, *P. hamadryas*, Napier (1981); *M. fascisularis*, *M. mulatta*, Fooden (2006); *M. radiata*, *M. assamensis*, Fooden (1988); *M. nemestrina*, Fooden (1975). These specimens are housed at the Natural History Museum, London and Primate Research Institute of Kyoto University.

The precision of each model was evaluated by the adjusted R^2 and %SEE. The adjusted R^2 is calculated from the SEE (standard error of estimates) and the sample standard deviation as follows. The smaller SEE becomes, closer to one if the adjusted R^2 becomes more precise. The model follows from:

Assuming, measured value: x, estimated value: y, and sample size: n.
Then, SEE = sqrt [$\Sigma(x - y)^2 / (n-2)$].
The sample standard deviation of y (σy^2) = $\Sigma(y - ymean) / (n-1)$
Adjusted $R^2 = (\sigma y^2 - SEE^2) / \sigma y^2$

The %SEE (SEE / the average of estimated values x 100%) of each model was also calculated and the results are shown in Table 5. The estimated values of these 15 species were plotted (Y) on the real values (X) in scatter plots (Figure 2). The precision of the

estimated values was evaluated by using the 95% confidence interval (CI). In Figure 2, the reference line (X-Y) was drawn with the 95% CI (x ±1.96 SEE). If the values are plotted over the maximum limit of the CI or under the minimum limit, then the values can be considered over- or underestimated, respectively.

Statistical analyses were performed using R software version 2.9 (R Development Core Team, 2009).

RESULTS

Predictive models using the measurements standardized by GMscra

Out of 10 measurements which had positive moderate correlation ($r > 0.5$) with RTL, 4 measurements were selected for multiple regression analyses. Two variables were from the sacrum (measurements No.8, No.12) and two from Ca2 (measurements No.17, No.18) (Table 1). Using these measurements, a total of seven predictive models were produced (Table 5).

Table 3 around here

The best-fit regression formula selected by the step-wise method was model 1 (adjusted R^2 = 0.64) (Figure 2, Table 5). This model used measurement No. 8 (sagittal diameter of the caudal articular surface of the sacrum), No. 12 (inter-postzygapophyseal breadth of the sacrum), and No. 17 (breadth at the transverse process of Ca2) to predict tail length. The SPRCs were 8.233 for No. 12, 6.981 for No. 8, and 3.313 for No. 17.

Model 2 was obtained using the same sacral measurements reported in model 1

(adjusted R^2 = 0.65) (Figure 2, Table 5). The SPRCs were 9.828 for No. 8 (sagittal diameter of the caudal articular surface of the sacrum) and 8.168 for No. 12. (inter-postzygapophyseal breadth of the sacrum)

Models 3 and 4 were univariate regression models using sacral measurements No. 8 (sagittal diameter of the caudal articular surface of the sacrum) and No. 12 (inter-postzygapophyseal breadth of the sacrum), respectively. The adjusted R^2 values of model 3 and model 4 were 0.50 and 0.42.

In order to check the possibility of tail length estimation from caudal vertebrae, Models 5 through 7 were calculated from the breadth of the transverse process and length of the vertebral body for each of the proximal caudal vertebrae (Table 5). The adjusted R^2s of models 5, 6, and 7 were moderately high. The highest (0.56) was from Ca1.

Table 4 around here

Predictive models using the indices

Table 4 shows the correlation matrix of the 18 indices and RTL. Six indices had moderate correlations (r > 0.5) with RTL. After eliminating SB3 (middle vs. caudal level sacral breadth) and TDSAS (cranial vs. caudal transverse diameter of the sacral articular surface), which were strongly correlated with SB2 and SDSAS respectively, five indices (SZL, SDSAS, MLDV, SB2, and VB13) were used for multiple regression analysis. Using these indices, eight models were produced (Table 5).

Table 5 around here

By the step-wise method, model 8, which uses four indices was selected. These indices include SZL (ratio of cranial vs. caudal inter-zygophyseal breadth of the sacrum), SB2 (cranial vs. caudal sacral breadth 2, see Table 2, Figure 1), SDSAS (cranial vs. caudal sagittal diameter of the sacral articular surface), and MLDV (mediolateral vs. dorsoventral breadth of the articular surface of the last sacral vertebra). The adjusted R^2 for model 8 was 0.69 and the SPRC of the variables was highest in SZL and lowest in MLDV. This model uses two indices (SDSAS and MLDV) reflecting the articular surface morphology of the last sacral vertebra. Therefore, two derivative models from this original model were calculated by dropping one of the two indices (model 9 without MLDV and model 10 without SDSAS). The adjusted R^2 (0.70) for model 9 is as high as that produced in model 8 (Table 5, Figure 1). This value represents the highest score for the predicting formulae obtained by this study (Table 4). The SPRCs for this model were 7.885 for SZL, 6.358 for SB2, and 4.833 for SDSAS (Table 5). The adjusted R^2 of model 10 was 0.68, and slightly lower than that of models 8 and 9. The SPRC was lowest for MLDV as is in model 8.

Univariate regression formulae (models 11, 12, 13, 14, 15) were calculated from SDSAS, SZL, SB2, MLDV, and VB13 (length of the vertebral body of 3rd caudal vertebra compared to 1st caudal vertebra). The adjusted R^2s of these models were 0.46, 0.46, 0.54, 0.28, and 0.21 respectively (Table 5). The adjusted R^2 was the highest in model 13 among these five formulae, but the predictive power of these formulae was relatively low. By comparison of the adjusted R^2 between model 11 and 14, it is apparent that MLDV's explanation power of RTL is much lower than that of SDSAS. VB13 is the only index from the proximal caudal vertebrae among the selected indices. The adjusted

R^2 of the formula using VB13 is low (0.21).

Application

To examine the utility of the obtained models, five formulae (adjusted R^2 >0.60) were selected (models 1, 2, 8, 9, 10) and applied to 15 catarrhine species/subspecies (Table 1, Figure 2). The average RTL values were different between sexes in the catarrhine species, therefore the values for males and females were plotted separately in order to check the utility exactly (only males were available for *Papio anubis* and *Macaca arctoides*). The X-Y reference line and lines showing the 95% CI were drawn. The vertical dashed lines show the range of the "short"-tailed category in Russo and Shapiro (2011) and the vertical solid lines show the RTL range of the hybrid macaques used in the present study. Generally, the predicted values for taxa that had RTLs within the range of 18.3 through 88.8% were plotted within 95% CI. Species whose RTL exceeded the range of the hybrid macaques were underestimated. All models seemed to predict everything as around 100 when the species whose RTL is more than 100% were applied. On the other hand, the RTL was overestimated in stump-tailed macaque (*Macaca arctoides*) with a diminutive tail.

Figure 2 around here

DISCUSSION

Tail reduction has occurred in various primate taxa. The greatest example of tail reduction is, of course, observed in hominoids, where all extant members have no tail.

Some functional and phylogenetical features which might affect tail reduction have been proposed, but the evolutionary process has not been clarified in any lineage since fossils documenting the tail reduction process have not been found. It is certain that future discoveries of fossils will reduce these gaps in the primate fossil record. However, given the rarity of caudal vertebrae preservation in the primate fossil record, it remains important to develop a method that predicts tail length from other aspects of skeletal morphology.

The predicting formulae were devised from hybrid macaques possessing three sacral vertebrae. Therefore, these formulae should be applicable for species with a "monkey-like" sacrum (three or four sacral vertebrae). Deriving these models from a phylogenetically narrow sample does not, however, limit the utility of this study. In fact, Rose et al. (1996) inferred that the tailless *Nacholapithecus kerioi* had fewer sacral vertebrae, a trait suggesting greater similar to monkeys.

This study also differs from similar previous attempts in two respects. First, subjects were controlled with respect to phylogenetic factors by using Japanese-Formosan hybrid macaques and excluding potentially integrated traits as much as possible. Moreover, RTLs of the hybrids varied serially from 18.3 to 88.8 %. Therefore, tail length associated morphological variation detected in this study retains a great functional quality, while minimizing phylogenetic influence and is likely close to the general tendency in catarrhines. Second, tail length was estimated quantitatively among catarrhines with an intermediate tail length (15.0 < RTL < 100.0 %). In previous studies, these catarrhines were lumped together as a single group ("reduced tail" or "short") and intra-group differences were not analyzed (Ankel, 1965, 1972; Russo and Shapiro, 2011; Ward *et al.*, 1991). Results from this study demonstrate that it is possible to

estimate tail length with reasonable accuracy in catarrhines in this range (except diminutive-tailed species).

Skeletal morphological parameters that strongly reflect tail length were identified in the sacrum and proximal caudal vertebrae. It might be expected that formulae using both the sacrum and caudal vertebral measurements would perform well. While this is true, reliable formulae (adjusted $R^2 > 0.60$) are also obtained from only the sacral measurements. This is a promising result for studies of fossils, since fossil sacral specimens are not frequently associated with proximal caudal vertebrae. Compared to the sacrum, the number of parameters defined in the proximal caudal vertebrae were fewer, so this is not to say that the proximal caudal vertebrae cannot serve as a good key to estimate tail length (for example, see model 5), but instead to highlight the predictive value of sacral measurements. Future studies may succeed in finding key features of the proximal caudal vertebrae for tail length estimation (either quantitative or categorical) (see Nakatsukasa *et al.*, 2004). However, it is noted that at least the axial length ratio between the proximal caudal vertebrae (or relative elongation of the Ca3 vertebral body) was a weak predictor of tail length if it is applied to catarrhines with intermediate length of tails (model 13).

Several measurements of the last sacral vertebra [inter-postzygapophyseal breadth (No.12), sagittal diameter of the caudal articular surface (No.8), and breadth at the transverse process (No.11)] are functionally related to tail length (models 1, 2, 8, 9, 10). Inter-postzygapophyseal breadth likely reflects the rigidity for withstanding stresses induced by movements of a tail. This might be parallel to the relative narrowing of the caudal surface of the last sacral vertebra in shorter-tailed and tailless catarrhines (Ward *et al.*, 1991). In macaques, no caudal muscles originate at the transverse process of the

last sacral vertebra, but muscle bundles originating from the vertebral column and os coxa converge and pass on the ventral and dorsal sides of the transverse process (Tojima, 2010). The transverse process of the last sacral vertebra appears to serve an important function for maintaining the muscle bundles and tendons passing through on it (Tojima, 2010). Among *Macaca* species which differ markedly in tail length, the difference of the caudal musculature development with tail length is more marked in the extensors and abductors (MM. extensor caudae lateralis, extensor caudae medialis, abductor caudae lateralis, abductor caudae medialis) compared to the flexors (MM. flexor caudae longus, flexor caudae brevis, iliocaudalis, pubocaudalis, ischiocaudalis) (Tojima, 2010). In longer tailed species, many researches clarified that extension of tail seemed to have important function during they are moving around the arboreal environment. Wilson (1972) and Larson and Stern (2006) described that primate tail played an important role of balance maintenance in arboreal environment. Some behavioral study observed that arboreal primates held their tails in extended position during quadrupedal walking (Bernstein *et al*., 1978; Stevens *et al*., 2008). In addition, it is found that extension of the tail serves to reorient the body during leaping by counteracting the angular momentum produced by pelvic rotation during takeoff from horizontal substrates (Emerson, 1985; Günther *et al.*, 1991; Essner, 2002). Dunbar and Badam (2000) reported that long tail of *Macaca radiata* have important prehensile and sensory functions in arboreal locomotion and posture. The transverse process of the last sacral vertebra seems to support these caudal muscles. In shorter-tailed species, some of the caudal muscles become tendinous before they pass by the last sacral vertebra. Russo and Shapiro (2011) also suggested that a lateral expansion of the transverse process may be related to an increase in the leverage of the proximal tail's abductor musculature, and thus positively correlated with

tail length.

The sagittal diameter of the caudal articular surface of the sacrum is probably related to a reduction in tail mobility (Russo and Shapiro, 2011). These authors noted that the shape of this articular surface becomes more circular in longer-tailed cercopithecoids compared to reduced-tailed catarrhines and interpreted that a rounder morphology is related to a wide range of tail movements. As indicated, MLDV can predict RTL when it is used with the other indices in multiple regression formulae. However, the results of this study demonstrate that the sagittal diameter of the last sacral vertebra reflected RTL more strongly compared to the ratio of transverse vs. sagittal diameter. Sagittal diameter of the articular surface causes changes in its shape from elliptically to circularly, so in that mean, the results obtained in this study are consistent with previous findings (Russo and Shapiro, 2011). This measurement is also possible to reflect the difference of tail maintenance. In a troop of rhesus macaques, some individuals walking with their tail keeping erect observed (Altmann, 1962; Ojha, 1974). This behavior is observed in other macaque species with short and long tail (wild *Macaca fuscata*, Itani, 1954; wild *Macaca fascicularis*, the author's personal observation in 2010). The frequency, total time, and the reason of this behavior are not fully understood. But if this behavior is common in short- or long-tailed catarrhines, the last sacral vertebra receives larger moments of force because of the tail weight and the movements against gravity in sagittal direction in longer-tailed species. Relative diameter of sagittal direction is considered to become larger against the moment of force.

In order to test the utility of the formulae, this study calculated Ankel's (1965) sacral index in the examined hybrid macaques. Among the 89 hybrid macaque individuals, there were 67 for which all four of the measurements (No. 1, 2, 5, 6 in Figure 1) could

be obtained. Fifty-six out of 67 individuals fit into the “reduced tail” category (roughly corresponding to 19.7 - 44.4 % in RTL). Since the RTLs of the hybrid macaques ranged from 18.8 to 88.8 %, this result supports the utility of the sacral index as a predictor of RTL. However, the correlation between the sacral index and RTLs in this sample was low (r = 0.32). Thus, while this index would be applicable for broad comparisons, alternative methods like those devised in this study are necessary for finer-grained studies in “short” tailed catarrhines.

Ward *et al*. (1991) devised the tapering index to estimate tail length. It is not possible to compare this method with the one reported here. The method reported by Ward et al. (1991) requires measurements of the cranial and caudal articular surfaces of the last sacral vertebra. The materials used by this study were all adults and the last two sacral vertebrae are completely fused. Technically, it is almost impossible to collect these measurements accurately from completely fused sacra because the border between the cranial end of the last sacral vertebra and the caudal end of the forward sacral vertebra is often unclear.

Prediction models obtained by this study performed well for various catarrhines whose RTLs were within the range of the reference hybrid macaques and offered the following important observations:

1) The morphology of the last sacral vertebra was shown to be an important feature reflecting tail length quantitatively in catarrhines with intermediate length of tails.

2) Quantitative tail length estimation is possible in catarrhines with intermediate length of tails.

3) The methods derived by this study require only minimal measurements and are readily applicable to fossil specimens.

However, this study also revealed the difficultly in predicting very long or very short tail lengths by only using the formulae for catarrhines with intermediate tail lengths. The formulae tend to underestimate RTLs in long-tailed catarrhines and to overestimate RTLs in diminutive-tailed catarrhines. Perhaps other morphological traits (or different combination of traits) that were not used in this study are applicable for tail length variation in those categories. In this study, standard osteometric techniques were employed. However, future studies might be encouraged to adopt more fine-grained methods (e.g., using 3D-digitizer or photogrammetry) or more detailed analyses of the relationships between the morphology of the proximal caudal vertebrae and tail length.

Acknowledgements

The author is grateful to Yuzuru Hamada of the Primate Research Institute, Kyoto University for his permission to study the hybrid macaques and his helpful suggestions and comments, and to Paula Jenkins and Louise Tomsett of the Natural History Museum, London for their help in studying the skeletal collections under their care. Masato Nakatsukasa of the Laboratory of Physical Anthropology, Kyoto University and Toshio Mouri of the Primate Research Institute gave me important advice and suggestions for the revision of this paper. Yoshi Kawamoto of the Primate Research Institute, Kyoto University gave me important advice and information about the genetic features of these hybrids. Wataru Yano gave me important advice and information, particularly on the statistical analyses. This study was supported by the Cooperation Research Program of the Primate Research Institute, Kyoto University, and by the Global COE Program A06 of Kyoto University.

LITERATURE CITED

Akaike H. (1973) Information theory and an extension of the maximum likelihood principle. In: Petrov B.N. and Csaki F. (eds.), Second International Symposium on Information Theory. Akademiai Kiado, Budapest, pp. 267-281.

Altmann S.A. (1962) A field study of the sociobiology of rhesus monkeys, *Macaca mulatta*. Annals New York Academy of Sciences 102: 338-435.

Ankel F. (1965) Der canalis sacralis als indikator für die länge der caudalregion der primaten. Folia Primatologica 3: 263-276 (in German).

Ankel F. (1972) Vertebral morphology of fossil and extant primates. In: Tuttle R. (ed.), The Functional and Evolutionary Biology of Primates. Aldine, New York, pp. 223-240.

Bernstein P.L., Smith W.J., Karensky A., and Rosene K. (1978) Tail positions of *Cercopithecus aethiops*. Zeitschrift fur Tierpsychologie-Journal of Comparative ethology 46: 268-278.

Cant J.G., Youlatos D., and Rose M.D. (2001) Locomotor behavior of *Lagothrix lagothricha* and *Ateles belzebuth* in Yasunı´ National Park, Ecuador: general patterns and nonsuspensory modes. Journal of Human Evolution 41: 141-166.

Cant J.G., Youlatos D., and Rose M.D. (2003) Suspensory locomotion of *Lagothrix lagothricha* and *Ateles belzebuth* in Yasunı´ National Park, Ecuador. Journal of Human Evolution 44: 685-699.

Dunbar D.C. and Badam G.L. (2000) Locomotion and posture during terminal branch feeding. International Journal of Primatology 21: 649-669.

Emerson S.B. (1985) Jumping and leaping. In: Hildebrand M., Bramble D.M., Liem K.F., and Wake D.B. (eds.), Functional Vertebrate Morphology. Belknap press, Cambridge, pp. 58-72.

Essner Jr. R.L. (2002) Three-dimensional launch kinematics in leaping, parachuting and gliding squirrels. The Journal of Experimental Biology 205: 2469-2477.

Fooden J. (1975) Taxonomy and evolution of Liontail and Pigtail macaques (Primates: Cercopithecidae). Fieldiana Zoology 67: 1-169.

Fooden J. (1988) Taxonomy and evolution of the *Sinica* group of macaques: 6. interspecific comparisons and synthesis. Fieldiana Zoology 45: 1-44.

Fooden J. and Albrecht G.H. (1999) Tail-length evolution in *fascicularis*-group

macaques (Cercopithecidae: *Macaca*). International Journal of Primatology 20: 431-440.

Fooden J. (2006) Comparative review of *fascicularis*-group species of macaques (Primates: *Macaca*). Fieldiana Zoology 107: 1-43.

German R.Z. (1982) The functional morphology of caudal vertebrae in New World monkeys. American Journal of Physical Anthropology 58: 453-459.

Günther M.M, Ishida H., Kumakura H., and Nakano Y. (1991) The jump as a fast mode of locomotion in arboreal and terrestrial biotopes. Zeitschrift für Morphologie und Anthropologie 78, 341.

Hamada Y., Watanabe T., Chatani K., Hayakawa S., and Iwamoto M. (2005) Morphometriccal comparison between Indian- and Chinese-derived rhesus macaques (*Macaca mulatta*). Anthropological Science 113: 183-188.

Hamada Y., Suryobroto B., Goto S., and Malaivijitnond S. (2008a) Morphological and body color variation in Thai *Macaca fascicularis fascicularis* North and South of the Isthmus of Kra. International Journal of Ptimatology 29: 1271-1294.

Hamada Y., Mouri T., Kunimatsu Y., Chatani K., Yamamoto A., Goto S., and Kawamoto Y. (2008b) Morphological investigation of Japanese and Formosan macaques in Wakayama Prefecture 1: relationship between caudal length/caudal vertebral number and degree of admixture. In: Kawamoto Y. (ed.), Report of the Grant-in-Aid "Influence of introduced species in biodiversity: Synthetic study of hybrid macaques in Wakayama Prefecture (# 16310156). pp. 9-40 (in Japanese).

Itani J. (1954) Takasakiyama no saru. Kobunsya, Tokyo (in Japanese).

Kawamoto Y., Shirai K., Araki S., and Maeno K. (1999) A case of hybridization between the Japanese and Taiwanese macaques found in Wakayama Prefecture.

Primate Research 15: 53-60 (in Japanese).

Kawamoto Y., Ohsawa H., Nigi H., Maruhashi T., Maekawa S., Shirai K., and Araki S. (2001) Genetic assess of a hybrid population between Japanese and Taiwanese macaques in Wakayama Prefecture. Primate Research 17: 13-21 (in Japanese).

Kunimatsu Y., Yamamoto A. (2008) Dental morphology of a hybrid population between Japanese and Taiwanese macaques in Wakayama Prefecture, Japan. In: Kawamoto Y. (ed.), Report of the Grant-in-Aid "influence of introduced species in biodiversity: Synthetic study of hybrid macaques in Wakayama Prefecture (# 16310156). pp. 51-76 (in Japanese).

Larson S.G. and Stern J.T. Jr. (2006) Maintenance of above-branch balance during primate arboreal quadrupedalism: coordinated use of forearm rotators and tail motion. American Journal of Physical Anthropology 129: 71-81.

Lemelin P. (1995) Comparative and functional myology of the prehensile tail in New World monkeys. Journal of Morphology 224: 351-368.

Mouri T., Hamada Y., Kunimatsu Y., Yamamoto A., Chatani K., and Kawamoto Y. (2008) Temporal muscle lines of hybrid macaques (*Macaca fuscata* x *M. cyclopis*) from Wakayama. In: Kawamoto Y. (ed.), Report of the Grant-in-Aid "influence of introduced species in biodiversity: Synthetic study of hybrid macaques in Wakayama Prefecture (# 16310156). pp. 41-49 (in Japanese).

Nakatsukasa M., Tsujikawa H., Shimizu D., Takano T., Kunimatsu Y., Nakano Y., and Ishida H. (2003) Definitive evidence for tail loss in *Nacholapithecus*, an East African Miocene hominoid. Journal of Human Evolution 45: 179-186.

Nakatsukasa M., Ward C.V., Walker A., Teaford M.F., Kunimatsu Y., and Ogihara N. (2004) Tail loss in *Proconsul heseloni*. Journal of Human Evolution 46: 777-784.

Napier J.R. and Napier P.H. (1967) Handbook of living primates. Academic Press, London, New York.

Napier P.H. (1981) Catalogue of primates in the British Museum (Natural History) and elsewhere in the British isles, Part Ⅱ: Family Cercopithecinae. British Museum (Natural History), London.

Ohsawa H., Morimitsu Y., Kawamoto Y., Muroyama Y., Maekawa S., Nigi H., Tori H., Goto S., Maruhashi T., Nakagawa N., Nakatani J., Tanaka T., Hayakawa S., Yamada A., Hayaishi S., Seino H., Saeki M., Kawai S., Hagiwara H., Suzuki Ka., Suzuki Ku., Uetsuki S., Okano M., Okumura T., Yoshida A., and Yokoyama N. (2005) Population explosion of Taiwanese macaques in Japan. The Natural History Journal of Chulalongkorn University, Supplement 1: 55-60.

Ojha P.R. (1974) Tail carriage and dominance in the rhesus monkey, *Macaca mulatta*. Mammalia 38: 163-170.

Organ J.M. (2007) The functional anatomy of prehensile and nonprehensile tails of Platyrrhini (Primates) and Procyonidae (Carnivora). PhD dissertation. Johns Hopkins University School of Medicine, Baltimore, Maryland.

Organ J.M. (2010) Structure and function of platyrrhine caudal vertebrae. Anatomical Record 293: 730-745.

Rose M.D., Nakano Y., and Ishida H. (1996) *Kenyapithecus* postcranial specimens from Nachola, Kenya. African Study Monographs, Supplement 24: 3-56.

Rosenberger A.L. (1983) Tale of tails: parallelism and prehensility. American Journal of Physical Anthropology 60: 103-107.

Russo G. and Shapiro L. (2011) Morphological correlates of tail length in the catarrhine sacrum. Journal of Human Evolution, 61: 223-232.

Schmitt D., Rose M., Turnquist J.E., and Lemelin P. (2005) Role of the prehensile tail during ateline locomotion: experimental and osteological evidence. American Journal of Physical Anthropology 126: 435-446.

Sokal R.R. and Rohlf F.J. (1995) Biometry. W. H. Freeman and Company, New York.

Stevens N.J., Wright K.A., Covert H.H., and Nadler T. (2008) Tail posture of four quadrupedal leaf monkeys (*Pygathrix nemaeus*, *P. cinerea*, *Trachypithecus delacouri* and *T. hatinhensis*) at the Endangered Primate Rescue Center, Cuc Phuong National Park, Vietnam. Vietnamese Journal of Primatology 2: 13-24.

Tojima S. (2010) Comparative anatomy of caudal musculature attachments between Formosan rock macaques (*Macaca cyclopis*) and rhesus macaques (*Macaca mulatta*). Primate Research 26: 107-113 (in Japanese).

Ward C.V., Walker A., and Teaford M.F. (1991) Proconsul did not have a tail. Journal of Human Evolution 21: 215- 220.

Wilson R.D. (1972) Tail reduction in *Macaca*. In: Tuttle R. (ed.), The Functional and Evolutionary Biology of Primates. Aldine, New York. pp. 241-261.

Youlatos D. (1998) Seasonal variation in the positional behavior of red howling monkeys (*Alouatta seniculus*). Primates 39: 449–457.

Youlatos D. (2002) Positional behavior of black spider monkeys (*Ateles paniscus*) in French Guiana. International Journal of Primatology 23: 1071–1093.

Zapfe H. (1958) The skeleton of *Pliopithecus* (*Epipliopithecus*) *vindobonensis* Zapfe and Hurzeler. American Journal of Physical Anthropology 16: 441-457.

Figure 1. Measurements taken: **A,** cranial articular surface of the sacrum (1: sagittal diameter of the sacral canal cranial opening, 2: transverse diameter of the sacral canal cranial opening, 3: transverse diameter of the cranial articular surface, 4: sagittal diameter of the cranial articular surface); **B,** caudal articular surface (5: sagittal diameter of the sacral canal caudal opening, 6: transverse diameter of the sacral canal caudal opening, 7: transverse diameter of the caudal articular surface, 8: sagittal diameter of the caudal articular surface); **C,** dorsal view of the sacrum (9: cranial breadth of the sacrum, 10: inter-prezygapophyseal breadth, 11: breadth at the transverse process of the last sacral vertebra, 12: inter-postzygapophyseal breadth); **D,** ventral view of the sacrum (13: ventral length, 14: middle breadth); **E,** dorsal view of the proximal caudal vertebrae (15: breadth at the transverse process (1st caudal vertebra), 17: breadth at the transverse process (2nd caudal vertebra), 19: breadth at the transverse process (3rd caudal vertebra)); **F,** lateral view of the proximal caudal vertebrae (16: length of the vertebral body (1st caudal vertebra), 18: length of the vertebral body (2nd caudal vertebra), 20: length of the vertebral body (3rd caudal vertebra))

Figure 2. The results of model 1 (A), 2 (B), 8 (C), 9 (D), and 10 (E) (Table 5) applied to catarrhine samples. The solid line is the X-Y reference line and the two dashed lines enclosing the reference line show the 95% confidence limits. The plotted numbers are the same as in Table 1. The results for males and females were plotted separately (male: diamonds; female: circles). The two vertical lines show the RTL variation of the hybrid macaques and the vertical dashed lines show the “short” category in Russo and Shapiro (2011).

Figure 1.

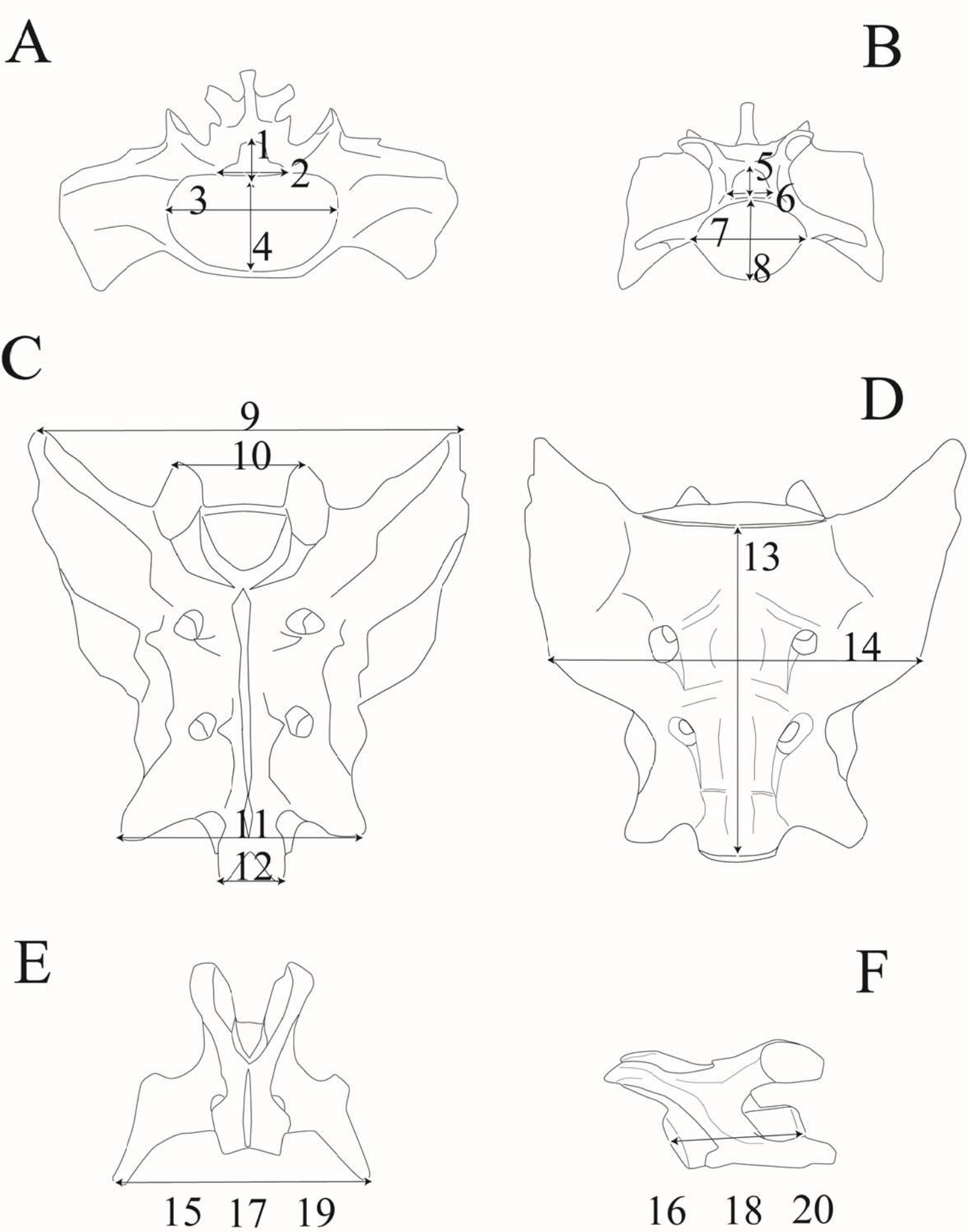

Figure 2.

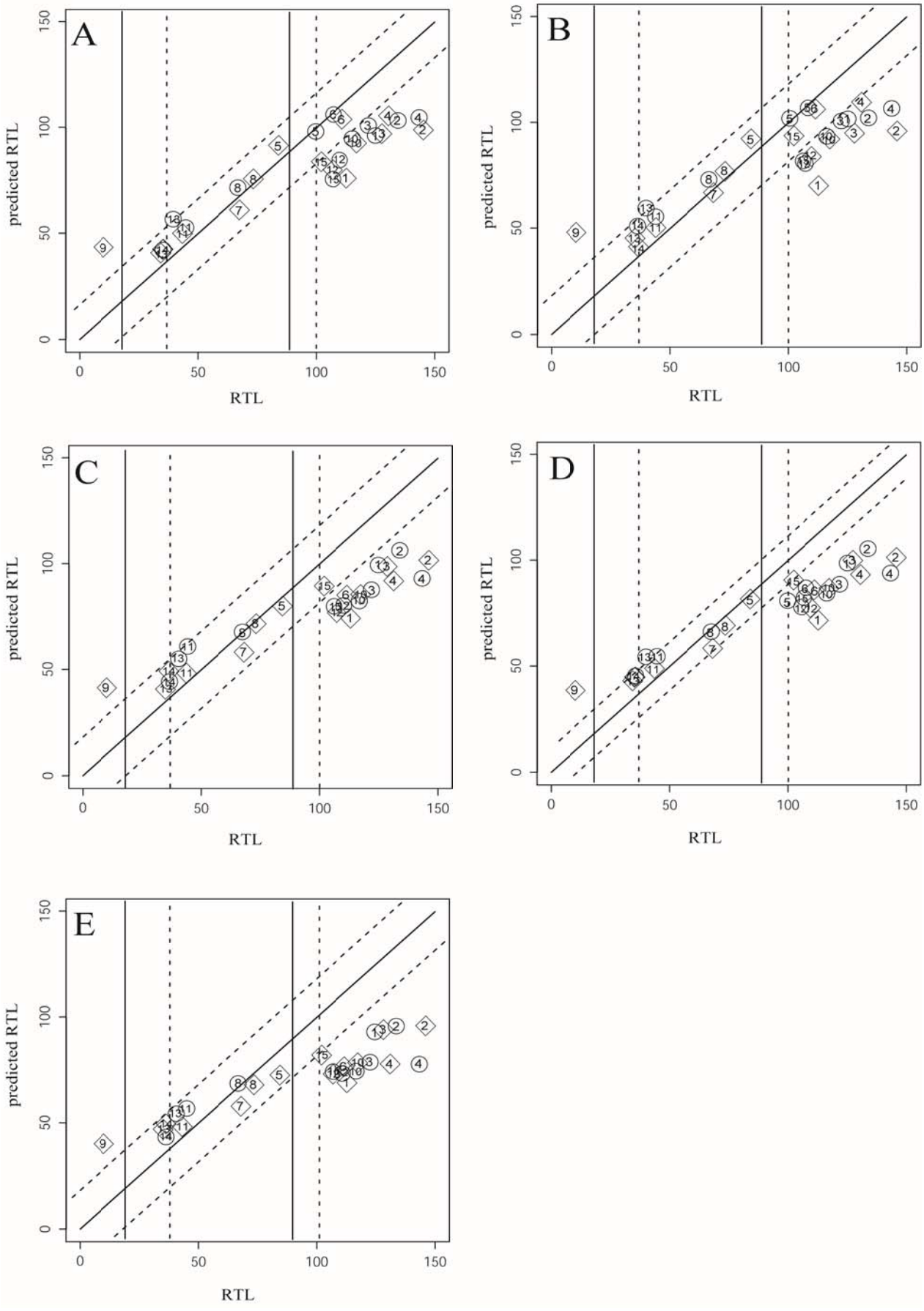

Table 1. Specimens used in this study

No.[a]	Taxon	Sex	N	Mean RTL (%)	RTL (%)
	Hybrid macaque	M	30	-	18.3-88.8 [b]
		F	58	-	18.9-87.2 [b]
		NA	1	-	(38.9 [b])
1	*Cercopithecus mitis kolbi*	M	1	113.2 [b]	
		F	3	124.9 [b]	
2	*Cercopithecus mitis stuhlmanni*	M	3	145.6 [b]	
		F	2	140.0 [b]	
3	*Cercopithecus neglectus*	M	2	127.8 [b]	
		F	1	122.2 [b]	
4	*Cercopithecus aethiops*	M	2	131.0 [b]	
		F	2	143.4 [b]	
5	*Erythrocebus patas*	M	2	84.2 [c]	
		F	3	100.0 [c]	
6	*Cercocebus torquatus*	M	1	111.5 [d]	
		F	1	108.5 [d]	
7	*Papio anubis*	M	1	68.0 [b]	
8	*Papio hamadryas*	M	10	73.3 [c]	
		F	7	67.2 [c]	
9	*Macaca arctoides*	M	1	10.3 [d]	
10	*Macaca fascicularis*	M	10	117.6 [e]	
		F	14	116.3 [e]	
11	*Macaca mulatta*	M	11	43.3 [e]	
		F	10	44.0 [e]	
12	*Macaca radiata*	M	10	107.0 [f]	
		F	7	110.0 [f]	
13	*Macaca assamensis*	M	5	35.0 [f]	
		F	4	40.0 [f]	
14	*Macaca nemestrina*	M	6	36.5 [g]	
		F	10	36.5 [g]	
15	*Colobus guereza*	M	2	102.2 [b]	
		F	2	106.7 [b]	

[a] Not including the hybrids, 15 species/subspecies were used.

[b] Field record associated with a skeleton; [c] Napier (1981); [d] Measured from the associated skin; [e] Fooden (2006); [f] Fooden (1988); [g] Fooden (1975).

Table 2. Calculated indices

Index	Abbreviation	Definition [a]
Transverse diameter of the sacral canal (cranial sacral vertebra vs. caudal sacral vertebra)	TDSC	No.6/No.2
Sagittal diameter of the sacral canal (cranial sacral vertebra vs. caudal sacral vertebra)	SDSC	No.5/No.1
Transverse diameter of the sacral articular surface (cranial sacral vertebra vs. caudal sacral vertebra)	TDSAS	No.7/No.3
Sagittal diameter of the sacral articular surface (cranial sacral vertebra vs. caudal sacral vertebra)	SDSAS	No.8/No.4
Mediolateral and dorsoventral breadth of the articular surface of the last sacral vertebra	MLDV	No.7/No.8
Inter-zygagophyseal breadth of the sacrum (cranial sacral vertebra vs. caudal sacral vertebra)	SZL	No.12/No.10
Sacral breadth 1 (cranial vs. middle level)	SB1	No.14/No.9
Sacral breadth 2 (cranial vs. caudal level)	SB2	No.11/No.9
Sacral breadth 3 (middle vs. caudal level)	SB3	No.11/No.14
Breadth at the transverse process (last sacral vertebra vs. 1st caudal vertebra)	LSTP1	No.15/No.11
Breadth at the transverse process (last sacral vertebra vs. 2nd caudal vertebra)	LSTP2	No.17/No.11
Breadth at the transverse process (last sacral vertebra vs. 3rd caudal vertebra)	LSTP3	No.19/No.11
Breadth at the transverse process (1st caudal vertebra vs. 2nd caudal vertebra)	TP12	No.17/No.15
Breadth at the transverse process (1st caudal vertebra vs. 3rd caudal vertebra)	TP13	No.19/No.15
Breadth at the transverse process (2nd caudal vertebra vs. 3rd caudal vertebra)	TP23	No.19/No.17
Length of the vertebral body (1st caudal vertebra vs. 2nd caudal vertebra)	VB12	No.18/No.16
Length of the vertebral body (1st caudal vertebra vs. 3rd caudal vertebra)	VB13	No.20/No.16
Length of the vertebral body (2nd caudal vertebra vs. 3rd caudal vertebra)	VB23	No.20/No.18

[a] For measurements, see Fig. 1.

Table 3. Correlation matrix of RTL and standardized measurements by GM (bold type: the correlation coefficient of candidates of variables; *: variables.)

	No.1	No.2	No.5	No.6	No.7	No.8	No.9	No.10	No.11	No.12	No.13	No.14	No.15	No.16	No.17	No.18	No.19	No.20
RTL	0.34	0.43	0.20	0.41	**0.59**	**0.76***	0.15	-0.20	**0.73**	**0.61***	0.31	0.29	**0.65**	**0.56**	**0.63***	**0.69***	**0.74**	**0.69**
No.1	1.00	0.47	0.22	0.69	0.38	0.36	0.38	0.18	0.18	0.43	0.51	0.26	0.31	0.50	0.50	0.41	0.31	0.36
No.2		1.00	0.57	0.64	0.49	0.55	0.29	-0.14	0.46	0.20	0.47	0.44	0.59	0.43	0.61	0.54	0.50	0.58
No.5			1.00	0.22	0.43	0.38	0.07	-0.37	0.34	-0.08	0.31	0.26	0.36	0.23	0.34	0.25	0.35	0.32
No.6				1.00	0.40	0.52	0.29	-0.11	0.38	0.39	0.40	0.32	0.53	0.43	0.60	0.49	0.46	0.48
No.7					1.00	**0.81**	0.31	-0.15	**0.7**	**0.32**	0.48	0.29	**0.72**	**0.59**	**0.54**	**0.74**	**0.72**	**0.70**
No.8						1.00	0.30	-0.30	**0.81**	**0.47**	0.51	0.32	**0.80**	**0.62**	**0.65**	**0.78**	**0.82**	**0.82**
No.9							1.00	0.25	0.28	0.30	0.38	0.58	0.40	0.25	0.27	0.35	0.10	0.39
No.10								1.00	-0.27	0.05	-0.08	-0.09	-0.24	-0.04	-0.13	-0.17	-0.30	-0.28
No.11									1.00	**0.53**	0.39	0.36	**0.80**	**0.50**	**0.52**	**0.74**	**0.64**	**0.81**
No.12										1.00	0.24	0.21	**0.46**	**0.42**	**0.44**	**0.52**	**0.35**	**0.51**
No.13											1.00	0.46	0.57	0.66	0.57	0.65	0.38	0.67
No.14												1.00	0.56	0.23	0.46	0.39	0.14	0.48
No.15													1.00	0.49	0.71	0.76	0.61	0.81
No.16														1.00	**0.64**	**0.82**	**0.71**	**0.72**
No.17															1.00	**0.60**	**0.68**	**0.61**
No.18																1.00	**0.70**	**0.94**
No.19																	1.00	**0.61**
No.20																		1.00

Table 4. Correlation matrix of RTL and indices (bold type: the correlation coefficient of candidates of variables; *: variables.)

	TDSC	SDSC	TDSAS	SDSAS	MLDV	SZL	SB1	SB2	SB3	LSTP1	LSTP2	LSTP3	TP12	TP13	TP23	VB12	VB13	VB23
RTL	-0.30	0.06	**0.62**	**0.72***	**-0.58***	**0.67***	0.20	**0.73***	**0.67**	-0.47	-0.47	-0.19	-0.26	0.14	0.40	0.46	**0.51***	0.41
TDSC	1.00	-0.24	-0.10	-0.21	-0.31	-0.26	-0.01	-0.09	-0.09	-0.03	0.01	0.02	0.05	0.04	0.00	-0.28	-0.26	-0.14
SDSC		1.00	0.07	0.06	-0.63	0.05	0.17	0.25	0.20	-0.09	-0.18	-0.09	-0.22	-0.03	0.13	0.26	0.28	0.17
TDSAS			1.00	**0.73**	0.36	**0.38**	0.04	**0.67**	**0.67**	-0.40	-0.54	-0.19	-0.48	0.10	0.49	0.56	**0.57**	0.37
SDSAS				1.00	-0.32	**0.54**	0.03	**0.69**	**0.69**	-0.41	-0.48	-0.16	-0.36	0.14	0.46	0.48	**0.55**	0.44
MLDV					1.00	-0.53	-0.07	-0.51	-0.49	0.36	0.37	0.19	0.23	-0.05	-0.26	-0.38	-0.54	-0.56
SZL						1.00	0.06	**0.57**	**0.56**	-0.39	-0.45	-0.32	-0.29	-0.03	0.19	0.43	**0.47**	0.37
SB1							1.00	0.23	-0.10	0.09	0.02	-0.13	-0.09	-0.25	-0.19	0.14	0.23	0.28
SB2								1.00	**0.94**	-0.77	-0.82	-0.53	-0.51	0.01	0.40	0.55	**0.62**	0.49
SB3									1.00	-0.81	-0.85	-0.50	-0.49	0.09	0.47	0.52	0.56	0.41
LSTP1										1.00	0.85	0.50	0.22	-0.25	-0.44	-0.30	-0.36	-0.29
LSTP2											1.00	0.70	0.70	0.09	-0.40	-0.59	-0.61	-0.41
LSTP3												1.00	0.60	0.71	0.38	-0.50	-0.65	-0.62
TP12													1.00	0.50	-0.14	-0.70	-0.66	-0.38
TP13														1.00	0.78	-0.32	-0.45	-0.47
TP23															1.00	0.15	0.00	-0.23
VB12																1.00	0.88	0.42
VB13																	1.00	0.80
VB23																		1.00

Table 5. Prediction models

Model	Used bony element(s)	Adjusted R^2	%SEE	Models[a, b, c]
1	Sacrum and 2nd caudal vertebra	0.64	11.67	RTL=8.233 x No.8 + 6.981 x No.12 + 3.313 x No.17 – 50.643
2	Sacrum	0.65	12.24	RTL=9.828 x No.8 + 8.168 x No.12 – 50.557
3	Sacrum	0.50	11.63	RTL=13.494 x No.8 - 50.117
4	Sacrum	0.42	13.39	RTL=12.308 x No.12 - 51.126
5	1st caudal vertebra	0.56	16.62	RTL=9.921 x No.15 + 6.269 x No.16 - 50.082
6	2nd caudal vertebra	0.51	16.62	RTL=7.963 x No.17 + 7.320 x No.18 - 50.226
7	3rd caudal vertebra	0.49	11.32	RTL=8.350 x No.19 +6.457 x No.20 - 51.419
8	Sacrum	0.69	8.23	RTL=7.7591 x SZL + 6.2601 x SB2 + 4.4097 x SDSAS – 0.9741 x MLDV + 49.4459
9	Sacrum	0.70	15.05	RTL=7.885 x SZL + 4.833 x SDSAS + 6.358 x SB2 - 49.437
10	Sacrum	0.68	8.98	RTL=8.661 x SB2 + 8.112 x SZL – 2.563 x MLDV + 49.476
11	Sacrum	0.46	13.13	RTL=12.983 x SDSAS - 50.111
12	Sacrum	0.46	13.47	RTL=12.972 x SZL - 51.161
13	Sacrum	0.54	10.40	RTL=14.648 x SB2 - 49.584
14	Sacrum	0.28	18.57	RTL= - 10.173 x MLDV + 49.976
15	1st and 3rd caudal vertebrae	0.21	17.60	RTL=8.484 x VB13 - 52.049

[a] For measurements and indices, see Figure 1 and Table 3, respectively.

[b] The measurements used in models 1 to 7 are all standardized by the GMscra.

[c] The coefficients of these models are SPRCs.